PCCP

PAPER

View Article Online
View Journal | View Issue

Cite this: *Phys. Chem. Chem. Phys.*, 2021, **23**, 10629

Formation of water-in-oil microemulsions within a hydrophobic deep eutectic solvent†

Divya Dhingra,[a] Kamalakanta Behera,[b] Bhawna[a] and Siddharth Pandey *[a]

Received 31st December 2020,
Accepted 9th April 2021

DOI: 10.1039/d0cp06716d

rsc.li/pccp

Hydrophobic deep eutectic solvents (DESs) as neoteric, non-toxic, and inexpensive media have the potential to replace organic solvents in various aggregation processes. Conventional water-in-oil microemulsions are formed using mostly environmentally unfavorable toxic organic solvents as the bulk oil phase. Evidence of formation of water-in-DES microemulsions is presented. These novel assemblies are formed using a hydrophobic DES constituted of *n*-decanoic acid (DA) and tetra-*n*-butylammonium chloride (TBAC) in 2 : 1 mole ratio, termed TBAC-DA, as the bulk oil phase. It is observed that in the presence of a common and popular non-ionic surfactant Triton X-100 (TX-100), water pools are formed within TBAC-DA under ambient conditions with maximum water loading (w_0 = [water]/[TX-100]) of 60 ± 3 for [TX-100] = 300 mM. The formation of the microemulsions is established by using fluorescence probe pyranine, which exhibited the appearance of a band characterizing the un-protonated form of the probe clearly implying onset of water-in-TBAC-DA microemulsion formation. The UV-vis absorbance of Co^{II} further corroborates TX-100-assisted water pool formation within TBAC-DA *via* the appearance of the band that is assigned to the response of the probe in water. Dynamic light scattering (DLS) measurement suggests average aggregate sizes to be in the range of 72(±4) to 122(±7) nm. These unprecedented water-in-DES microemulsions may have far reaching implications due to their benign nature.

Introduction

Microemulsions have emerged as a versatile reaction media since their discovery in 1959.[1] They can be well defined as isotropic, optically transparent and thermodynamically stable dispersions consisting of two or more immiscible liquids (generally a polar and a non-polar component) stabilized by an emulsifying agent, preferably a surfactant, at the liquid–liquid interface.[2,3] Microemulsions have been an interesting subject of research as they offer the significant advantages of compartmentalized species with easy formation, low cost preparation, thermodynamic stability, high efficiency, homogeneity, and improved bioavailability.[1–3] They have found potential applications in a variety of disciplines, such as, biochemistry, nanotechnology, synthesis, extraction, separation, oil recovery, polymerization and in the pharmaceutical, cosmetic, agrochemical, and food industries.[1,4–6] Depending on the nature and proportion of the constituting solvents, these aggregates may be characterized as oil-in-water microemulsions or water-in-oil microemulsions, wherein water is the polar phase and a hydrophobic toxic organic solvent is usually the oil phase.[1,2]

The conventional organic solvents used as oil phase (*e.g.*, benzene, toluene, carbon tetrachloride, cyclohexane, iso-octane, *n*-octane, and ethyl acetate, among others) are usually highly volatile, toxic and cause detrimental effects to the environment and human health[7,8] apart from offering a limited range in physicochemical properties. Owing to their inherent nature, the conventional water-in-oil microemulsions that contain large amounts of organic solvents as the bulk phase have restricted practical applications. Considering the importance and widespread usage of microemulsions in various industries, it is necessary to find a sustainable and greener alternative for toxic organic solvents in order to make eco-friendly microemulsion systems, thus, exploiting the great advantages these microemulsions offer, while keeping in mind the green chemistry agenda. In this regard, several groups have reported the use of water-immiscible ionic liquids (ILs) as the oil phase in the formation of water-in-oil microemulsions.[9–11] Though ILs have emerged as potential replacements to the conventional organic solvents as the bulk oil phase in these water-in-IL microemulsions, there are several concerns regarding their high cost, major toxicity, hydrolytic instability, environmental incompatibility, and non-sustainability, among others.[12] Their role as an effective substitute for conventional organic solvents in microemulsion formation is clearly compromised.

[a] *Department of Chemistry, Indian Institute of Technology Delhi, Hauz Khas, New Delhi – 110016, India. E-mail: sipandey@chemistry.iitd.ac.in; Fax: +91-11-26581102; Tel: +91-11-26596503*
[b] *Department of Applied Chemistry (CBFS-ASAS), Amity University, Gurugram, Manesar, Panchgaon, Haryana 122413, India*

† Electronic supplementary information (ESI) available. See DOI: 10.1039/d0cp06716d

The emergence of deep eutectic solvents (DESs) in recent years has afforded a neoteric route in the formation of various aggregate assemblies.[12,13] DESs are proving to be environmentally-benign and inexpensive alternatives to both organic solvents and ILs.[14–16] Similar to ILs, DESs also exhibit favourable physicochemical properties, such as negligible vapour pressure, low volatility, a wide electro-chemical window, non-flammability, high thermal stability, and a wide liquid range.[12–15] In addition, their low cost, environmentally-benign nature, and ease in the tailorability of their physical properties have led to their exploration in numerous applications in chemical industries, in polymer science, in nanomaterial fabrication, and as reaction media, to name a few.[12–15] As the majority of the DESs reported in the literature are hydrophilic in nature, there have been obvious attempts at employing them in the formation of direct micelles,[17–19] DES-in-oil microemulsions[20] and oil-in-DES microemulsions,[19] where a hydrophilic DES replaces water as the polar phase. However, a conventional organic solvent, which is mostly toxic in nature, is still a major constituent of many of such systems. The recent advent of hydrophobic DESs[21–26] has afforded an opportunity to form water-in-oil microemulsions by replacing toxic organic solvents with hydrophobic DESs as oil phase, thus creating water pools within a non-toxic and inexpensive hydrophobic DES as the bulk phase. Hydrophobic DESs belong to a new subclass of DESs, which uses H-bond donors (HBDs), such as monocarboxylic acids, menthol, thymol, and monoterpenes, among others, with quaternary ammonium/phosphonium salts as H-bond acceptors (HBAs).[21–26] So far, to the best of our knowledge, there exists only a single report involving formation of stable oil-in-water emulsion using a hydrophobic eutectic system composed of 1-tetradecanol and menthol in a 1 : 2 molar ratio.[27]

Herein, we report the very first example of water-in-DES microemulsions using a hydrophobic DES constituted of *n*-decanoic acid (DA) with tetra-*n*-butylammonium chloride (TBAC) in a 2 : 1 mole ratio, termed TBAC-DA from here-on, as the oil phase. This eutectic system is reported to exhibit a large depression in its melting point *i.e.*, $T_m \sim -11.9$ °C.[21] Several emulsifying surfactants are investigated with Triton X-100 (TX-100), a common non-ionic surfactant, being found as the most effective among them (structures are given in Fig. 1). The formation of the microemulsions is corroborated and characterized by using steady-state fluorescence, and UV-vis absorbance spectroscopies and conductivity. The size of microemulsion formed is measured using dynamic light scattering spectroscopy.

Results and discussion

We first examined the solubility of various common surfactants, namely SDS (anionic), CTAB (cationic), Brij-35 and TX-100 (both non-ionic), within neat DES TBAC-DA. It was observed that both the ionic surfactants, SDS and CTAB, were only sparingly soluble in TBAC-DA (<0.5 mM under ambient conditions). Non-ionic surfactant Brij-35 solidified within neat TBAC-DA under ambient conditions rendering it difficult to carry out any further investigation with SDS, CTAB, and Brij-35 as far as the formation of optically transparent aggregates is concerned. Non-ionic surfactant TX-100, on the other hand, exhibited close to complete miscibility within neat TBAC-DA under ambient conditions. It is noteworthy that most of the reports on water-in-IL microemulsions are on non-ionic surfactants; very few of the studies have reported the use of ionic or zwitterionic surfactants either in the absence or presence of cosurfactant/cosolvent/additive.[9,10,28] Furthermore, the observed surfactant solubility behaviour within hydrophobic DES TBAC-DA is well correlated to that for hydrophobic ILs underlining the role of hydrophobicity of the media in determining surfactant miscibility as ionic/polar substances tend to exhibit lesser or no miscibility in non-polar media, in general.

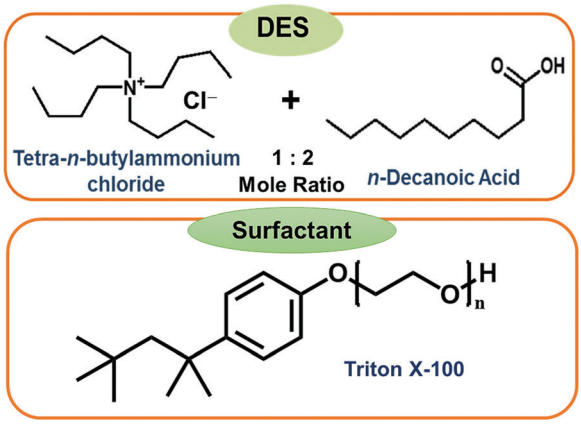

Fig. 1 Structures of the surfactant and components of DES TBAC-DA used in the study.

The maximum intake of water under ambient conditions by TBAC-DA in the absence of TX-100 is found to be *ca.* 5.8 M. We next assessed the water intake by TBAC-DA in the presence of varying concentrations of TX-100 under ambient conditions. Water miscibility is found to dramatically increase by increasing TX-100 concentration within TBAC-DA (Fig. 2). This implies possible formation of surfactant-assisted water pools within TBAC-DA akin to the traditional water-in-oil microemulsion formation with organic solvent being replaced by hydrophobic DES TBAC-DA as the bulk oil phase. As for the traditional

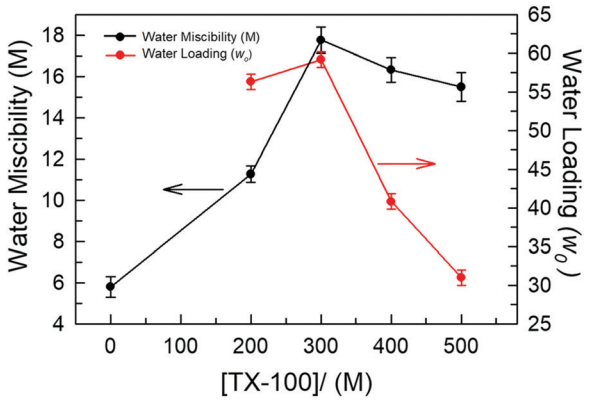

Fig. 2 Plots depicting water miscibility (*M*) and water loading (w_0) within the TX-100/TBAC-DA system for different concentrations of TX-100.

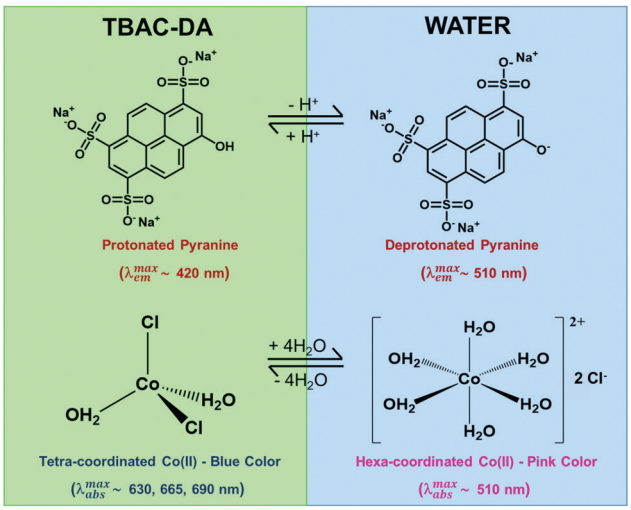

Fig. 3 Structures of various forms of pyranine and Co^{II} based on the solubilizing media.

water-in-oil microemulsions, these water-in-DES microemulsions would require the orientation of the polar head-group of the non-ionic surfactant to orient toward the water pool, whereas the hydrophobic surfactant long chain to be solubilized by the bulk hydrophobic DES. We next estimated the water loading (w_0), defined as w_0 = [water]/[TX-100], where [water] and [TX-100] are the molar concentrations of water and surfactant TX-100, respectively, for these water-in-DES microemulsions. We have found that under ambient conditions, w_0 initially increases with increase in TX-100 concentration, attains a maximum when [TX-100] ~ 300 mM and then decreases (Fig. 2). The physical state of TX-100 under ambient conditions is liquid. As the concentration of TX-100 within the system is increased, it may start to compete with the DES as the bulk liquid phase. This may also result in subsequent exchange of roles between TX-100 and *n*-decanoic acid (DA, the major component of the DES on molar basis), where a fraction of DA might start to act as the surfactant and a fraction of TX-100 as part of the oil phase, and thus the relevance of w_0 may be lost. Investigation to test this hypothesis is currently underway in our research laboratories. The formation of unprecedented water-in-DES microemulsions in the presence of low-to-moderate concentrations of TX-100 is evident nonetheless.

We validated the formation of these DES-based microemulsions using optical spectroscopic methods that are well established for such purposes.[1,10,11] We have carried out these investigations for microemulsions with different concentrations of TX-100 in TBAC-DA at 298.15 K. Fluorescence probe pyranine (structure provided in Fig. 3) has been effectively utilized by several groups to characterize reverse micelles and water-in-oil/water-in-IL microemulsions, among others.[29–31] The excited-state proton transfer (ESPT) reaction of pyranine does not take place in neat or water-saturated hydrophobic DES TBAC-DA (Fig. 4A). The steady-state fluorescence emission spectra of pyranine in neat TBAC-DA are characterized by the band centred at *ca.* 420 nm, which is due to the presence of the predominantly protonated form of pyranine in the solution.[30] As the intensity of the band increases with increase in the amount of water uptake, there is no change in the shape of the band and no new band appears either (Fig. 4B). This indicates that added water up to the miscibility limit in TBAC-DA forms a homogeneous solution, and is thus unable to initiate any

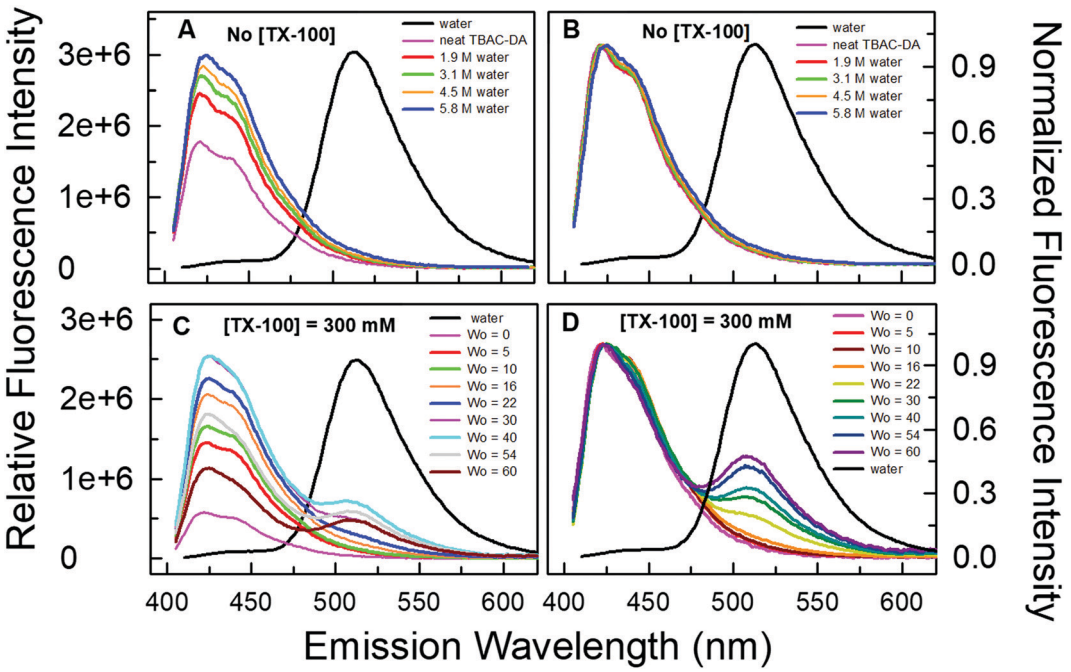

Fig. 4 Relative (panels A and C) and normalized (panels B and D) fluorescence emission spectra of pyranine (10 μM, λ_{ex} = 390 nm, and slits: excitation/emission = 2/2 nm) dissolved within neat DES TBAC-DA and TX-100(300 mM)/TBAC-DA systems at different amounts of water loading (w_0), respectively. The fluorescence emission spectrum of pyranine in water is also included in each panel for reference.

deprotonation of pyranine. Several authors have earlier reported the absence of ESPT reaction of pyranine within neat organic solvents and common ILs.[31–33] However, previous reports have shown that the ESPT reaction of pyranine takes place efficiently within the water-in-oil and water-in-IL microemulsions where the probe tends to preferentially locate within the water pools.[29–31] On similar lines, we have witnessed pyranine ESPT reaction occurring within TX-100-added TBAC-DA in the presence of varying amount of water quantized by different amounts of w_0. This is clearly indicated by the appearance of a new band at *ca.* 511 nm with simultaneous decrease in the intensity of the band at *ca.* 420 nm as the water content is increased within the (TX-100 + TBAC-DA) system (Fig. 4C and D and Fig. S1, ESI† show fluorescence emission spectra of pyranine dissolved in TBAC-DA with 200, 300 and 500 mM TX-100, respectively, in the presence of varying amounts of w_0). It is interesting to note that the appearance of the band depicting deprotonated pyranine (*i.e.*, the band at *ca.* 511 nm) starts for w_0 corresponding to water concentration just above the water miscibility limit (*ca.* 5.8 M, *vide supra*) of neat TBAC-DA ($w_0 > 25$, 16, and 11 for 200, 300, and 500 mM TX-100, respectively). It is envisaged that water-in-TBAC-DA microemulsions start to form in the presence of TX-100 as the added water becomes more than the miscibility limit of water in neat hydrophobic DES, thus preferentially solvating the pyranine within the water pools where the deprotonated form of the probe predominates. Formation of water-in-DES microemulsions is thus clearly corroborated.

Another optical spectroscopic method to establish the presence of water-in-oil microemulsions is based on the change in UV-vis absorbance spectrum of Co^{II} in going from predominantly tetra-coordinated Co^{II} in the oil phase (absorbance spectrum characterized by peaks at *ca.* 630, 665, and 690 nm affording blue colour to the solution) to hexa-coordinated Co^{II} in the aqueous phase (due to the presence of $[Co(H_2O)_6]^{2+}$, structure given in Fig. 3; absorbance spectral band at *ca.* 510 nm with pink colour solution).[10] The UV-vis absorbance spectra of Co^{II} in neat TBAC-DA and 5.8 M water solution in TBAC-DA, respectively, are characterized by peaks only at *ca.* 630, 665, and 690 nm for both solutions, clearly suggesting the homogenous nature of the water solution in TBAC-DA (Fig. 5A). The UV-vis absorbance spectra of Co^{II} within 200 mM TX-100 solutions of TBAC-DA in the absence and presence of water under ambient conditions clearly show the appearance of the band at *ca.* 510 nm as the concentration of water becomes higher than the water miscibility limit of TBAC-DA (Fig. 5B). This supports the proposition that excess water forms water pools with the help of surfactant TX-100 within hydrophobic DES TBAC-DA. The UV-vis absorbance of Co^{II} is amply able to establish the presence of water-in-DES microemulsions as well.

Furthermore, an estimate of the size of these novel water-in-DES microemulsions is obtained using the dynamic light scattering (DLS) technique as shown in Fig. 6. It is interesting to note that monomodal distribution is observed for each solution. The formation of large size aggregates (72–122 nm) indicates the formation of aggregated reverse micelle-like structures within the hydrophobic DES-based system at each concentration of

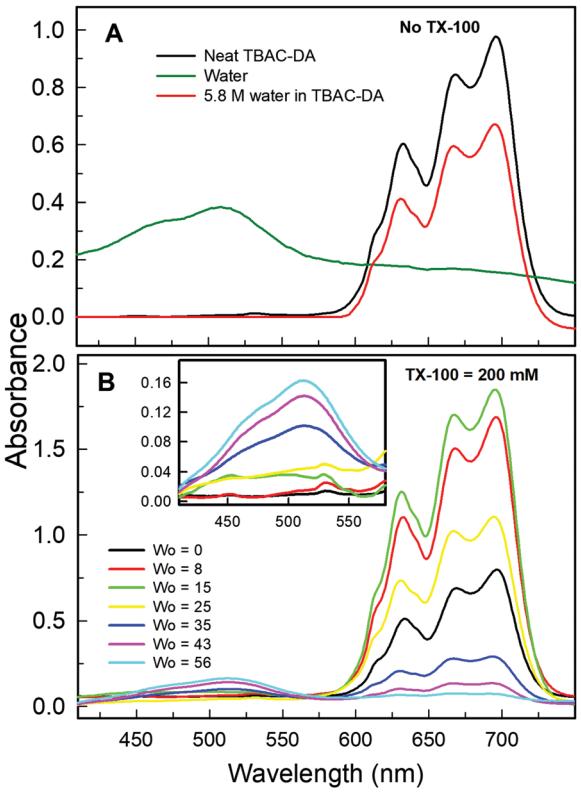

Fig. 5 UV-vis absorption spectra of Co^{II} within water, neat TBAC-DA, and water saturated TBAC-DA (panel A) and the TX-100 (200 mM)/TBAC-DA system (panel B) at different amounts of water loading (w_0). Inset in panel B is the magnified portion of the plot for clear depiction of the peak at ~509 nm.

TX-100. It is evident from the plots of normalized scattered intensities *versus* average particle diameter that there is an increase in the aggregate size as w_0 is gradually increased. This may be due to the formation of water pools within the water-in-DES microemulsions at higher w_0 values. It is noteworthy that the results obtained from DLS clearly support the UV-vis absorbance and fluorescence spectral responses where a new peak appears at higher water concentrations indicating the formation of water pools within the water-in-DES microemulsions.

We further characterized the phase behavior of microemulsions using electrical conductivity measurements. The concentration of TX-100 in TBAC-DA was fixed at 300 mM and water was added incrementally to the monophasic system up to w_0 = 101, beyond which it bifurcated into two layers. The electrical conductivity *versus* w_0 curve is used to identify the different microemulsion regions, *i.e.*, water-in-DES (A), bicontinuous (B), and DES-in-water (C) phase (Fig. 7). It is observed that in the absence of water, the electrical conductivity of TX-100/TBAC-DA is low (~0.08 mS cm^{-1}); it increases marginally upon initial addition of water. However, a substantial linear increase in electrical conductivity is observed as more water is added (up to w_0 = 60). Beyond this point, a non-linear increase in the electrical conductivity is obtained before it starts to decrease. The obtained results are in good agreement with those reported in the literature for typical non-aqueous microemulsions,[34,35] where the change in electrical conductivity

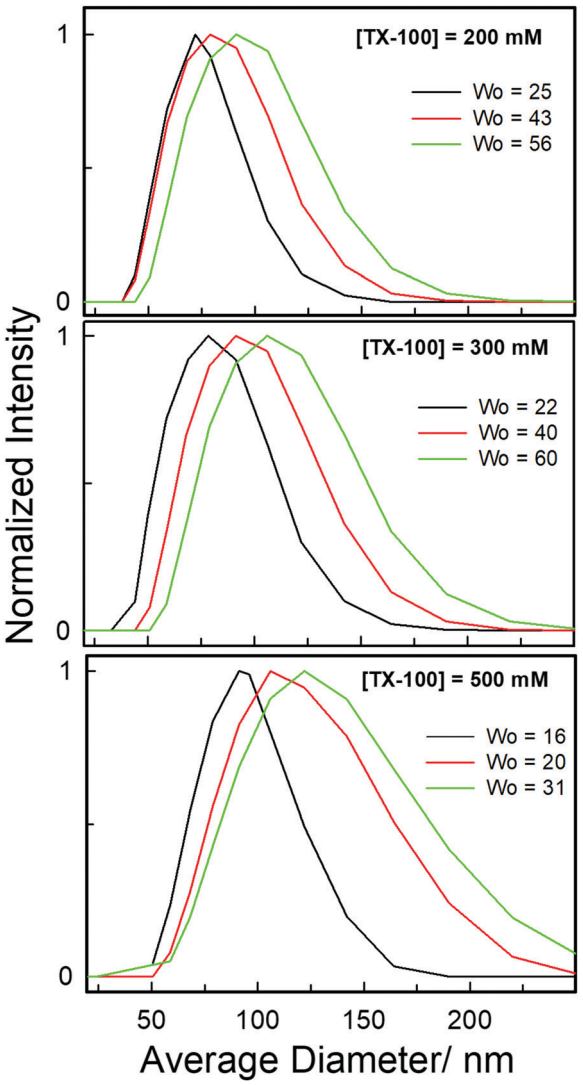

Fig. 6 Average size distribution of microemulsions formed within various TX-100/TBAC-DA systems at different amounts of w_0 obtained from DLS measurements at ambient conditions.

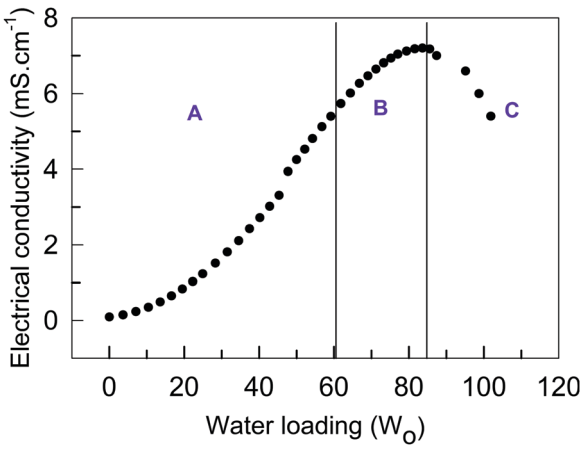

Fig. 7 Electrical conductivity (mS cm^{-1}) as a function of water loading (w_0) in water/TX-100 (300 mM)/TBAC-DA microemulsion at ambient conditions. Regions A, B, and C are described in the text.

is described in four stages as per the percolation phenomenon. Stage 1 is the initial increase in electrical conductivity arising from aggregation of inverse microemulsions followed by stage 2, which observes a linear increase in electrical conductivity due to the partial fusion of aggregated inverse micro-droplets, which leads to the formation of water-in-oil microemulsions. A non-linear increase in electrical conductivity is witnessed in stage 3, which arises from the growth and interconnection of the aqueous micro-domains leading to the formation of a bicontinuous phase. The oil/water microemulsion is formed in the final stage, characterized by a decrease in electrical conductivity. Therefore, the different sub-regions are conveniently located by electrical conductivity measurements.

Conclusion

In summary, we have presented the evidence for formation of water-in-oil microemulsions using a common non-ionic surfactant TX-100 and a representative hydrophobic DES TBAC-DA as the oil phase. Characterization of these unprecedented microemulsions is carried out using fluorescence from a suitable probe pyranine as well as UV-vis absorbance from Co^{II}. DLS and electrical conductance measurements further corroborate the presence of aggregates within the system. These novel assemblies formed using a non-toxic, readily available and neoteric DES in lieu of the conventional organic solvent as the oil phase may have far-reaching implications as far as various chemical and biotechnological applications requiring water-in-oil microemulsions are concerned.

Experimental

Materials

TBAC-DA was prepared by mixing tetra-*n*-butylammonium chloride (≥97% from Sigma-Aldrich) with *n*-decanoic acid (≥98% from Sigma-Aldrich) in a molar ratio of 1 : 2 followed by constant stirring and gentle heating (~40 °C) until a homogeneous, clear liquid was formed. The DES thus obtained was dried under vacuum for about 2 hours. The water content of the DES TBAC-DA was measured using a Karl Fischer titrator prior to its use and was found to be <100 ppm. Sodium dodecyl sulfate (SDS) was obtained from SISCO Research Laboratories; cetyltrimethylammonium bromide (CTAB) was obtained from CDH; TX-100 and Brij-35 were obtained from Sigma-Aldrich. All surfactants were used as received. Fluorescence probe pyranine [≥99.0% (GC), puriss for fluorescence] with the highest purity was obtained from Sigma-Aldrich Co. and stored under dry conditions. Absolute ethanol was used to prepare its stock solution. Cobalt(II) chloride hexahydrate was used as received from CDH. Doubly distilled deionized water of HPLC grade was obtained from Merck.

Methods

Surfactant solution of desired concentration was freshly prepared in TBAC-DA by constant shaking. The maximal water uptake was determined by visual cloud point observation. A precalculated

amount of the water was directly added to the surfactant solution of TBAC-DA to achieve the required water loading. Stock solution of pyranine was prepared by dissolving it in ethanol in pre-cleaned amber glass vials and stored at 4 ± 1 °C to retard any photochemical reaction. Samples for fluorescence data acquisition were prepared by taking appropriate aliquots of the probe from the stock and evaporating ethanol using a gentle stream of high purity nitrogen gas and adding the required amount of the solution to achieve the final probe concentration. Steady-state fluorescence spectra were acquired on a Jobin-Yvon Fluorolog-3 (model FL-3-11) modular spectrofluorometer equipped with a 450 W Xe arc lamp as the excitation source and single-grating monochromators as wavelength selection devices with a photomultiplier tube as the detector. Samples for UV-vis absorbance data acquisition were prepared by weighing an appropriate amount of cobalt(II) chloride and then adding the required amount of the solution to achieve the final probe concentration. A PerkinElmer Lambda 35 double beam spectrophotometer with variable bandwidth was used for the acquisition of the UV-vis molecular absorbance spectra. All spectra were duly corrected by subtracting the spectral responses from suitable blanks prior to data analysis. The dynamic light scattering (DLS) experiments were performed on a DelsaTM Nano C Particle Size Analyzer (Beckman Coulter, San Diego, CA, USA). It was equipped with a 658 nm laser diode operating at a 30 mW power output as the light source. All the DLS measurements were performed at a scattering angle of 165° under ambient conditions. Data analysis was performed using the SigmaPlot v10 software. All the data were acquired using 1 cm path length quartz cuvettes. All the measurements were taken in triplicate starting from the sample preparation and averaged. Conductivity measurements were carried out on a CM-183 μp-based EC-TDS analyzer with an ATC probe and conductivity cell (CC-03B) purchased from Elico Ltd, India.

Conflicts of interest

There are no conflicts to declare.

Acknowledgements

This work is generously supported by the Department of Science and Technology-Science & Engineering Research Board (DST-SERB), Government of India through a grant to Siddharth Pandey (grant number EMR/2016/005053).

References

1 A. K. Rakshit, B. Naskar and S. P. Moulik, Commemorating 75 Years of Microemulsion, *Curr. Sci.*, 2019, **116**, 898–912.
2 T. F. Tadros, *Applied Surfactants: Principle and Applications*, Wiley-VCH, Weinheim, 2005.
3 C. Solans and H. Kunieda, *Industrial Application of Microemulsions*, Marcel Dekker Inc., New York, 1997.
4 R. A. Martínez-Rodríguez, F. J. Vidal-Iglesias, J. Solla-Gullon, C. R. Cabrera and J. M. Feliu, Synthesis of Pt Nanoparticles in Water-in-Oil Microemulsion: Effect of HCl on Their Surface Structure, *J. Am. Chem. Soc.*, 2014, **136**, 1280–1283.
5 S. Asgari, A. H. Saberi, D. J. McClements and M. Lin, Microemulsions as Nanoreactors for Synthesis of Biopolymer Nanoparticles, *Trends Food Sci. Technol.*, 2019, **86**, 118–130.
6 E. Dickinson, Food Emulsions and Foams: Stabilization by Particles, *Curr. Opin. Colloid Interface Sci.*, 2010, **15**, 40–49.
7 P. T. Anastas, L. G. Heine and T. C. Williamson, *Green Chemical Syntheses and Processes: Introduction*, American Chemical Society, Washington, 2000, vol. 767, ch. 1, pp. 1–6.
8 C. Bolm, O. Beckmann and O. A. G. Dabard, The Search for New Environmentally Friendly Chemical Processes, *Angew. Chem., Int. Ed.*, 1999, **111**, 957–959.
9 M. Hejazifara, O. Lanaridia and K.-B. Schröder, Ionic Liquid Based Microemulsions: A Review, *J. Mol. Liq.*, 2020, **303**, 112264.
10 K. Behera, N. I. Malek and S. Pandey, Visual Evidence for Formation of Water-in-Ionic Liquid Microemulsions, *ChemPhysChem*, 2009, **10**, 3204–3208.
11 M. Moniruzzaman, N. Kamiya and M. Goto, Biocatalysis in Water-in-Ionic Liquid Microemulsions: A Case Study with Horseradish Peroxidase, *Langmuir*, 2009, **25**, 977–982.
12 Q. Zhang, K. D. O. Vigier, S. Royer and F. Jerome, Deep Eutectic Solvents: Syntheses, Properties and Applications, *Chem. Soc. Rev.*, 2012, **41**, 7108–7146.
13 E. L. Smith, A. P. Abbott and K. S. Ryder, Deep Eutectic Solvents (DESs) and Their Applications, *Chem. Rev.*, 2014, **114**, 11060–11082.
14 A. Paiva, R. Craveiro, I. Aroso, M. Martins, R. L. Reis and A. R. C. Duarte, Natural Deep Eutectic Solvents - Solvents for the 21st Century, *ACS Sustainable Chem. Eng.*, 2014, **2**, 1063–1071.
15 M. Francisco, A. V. D. Bruinhorst and M. C. Kroon, Low-Transition-Temperature Mixtures (LTTMs): A New Generation of Designer Solvents, *Angew. Chem., Int. Ed.*, 2013, **52**, 3074–3085.
16 Y. Chen, D. Yu, L. Fu, M. Wang, D. Feng, Y. Yang, X. Xue, J. Wang and T. Mu, The Dynamic Evaporation Process of the Deep Eutectic Solvent $LiTf_2N$:*N*-methylacetamide at Ambient Temperature, *Phys. Chem. Chem. Phys.*, 2019, **21**, 11810–11821.
17 T. Arnold, A. J. Jackson, A. Sanchez-Fernandez, D. Magnone, A. E. Terry and K. J. Edler, Surfactant Behavior of Sodium Dodecylsulfate in Deep Eutectic Solvent Choline Chloride/Urea, *Langmuir*, 2015, **31**, 12894–12902.
18 M. Pal, R. K. Singh and S. Pandey, Evidence of Self-Aggregation of Cationic Surfactants in a Choline Chloride + Glycerol Deep Eutectic Solvent, *ChemPhysChem*, 2015, **16**, 2538–2542.
19 M. Pal, R. Rai, A. Yadav, R. Khanna, G. A. Baker and S. Pandey, Self-Aggregation of Sodium Dodecyl Sulfate within (Choline Chloride + Urea) Deep Eutectic Solvent, *Langmuir*, 2014, **30**, 13191–13198.
20 M. Sakuragi, S. Tsutsumi and K. Kusakabe, Deep Eutectic Solvent-Induced Structural Transition of Microemulsions Explored with Small-Angle X-ray Scattering, *Langmuir*, 2018, **34**, 12635–12641.
21 D. J. G. P. Van Osch, L. F. Zubeir, A. Van Den Bruinhorst, M. A. A. Rocha and M. C. Kroon, Hydrophobic Deep Eutectic

Solvents as Water-Immiscible Extractants, *Green Chem.*, 2015, **17**, 4518–4521.

22 D. J. G. P. Van Osch, C. H. J. T. Dietz, J. Van Spronsen, M. C. Kroon, F. Gallucci and M. Van, Sint Annaland and R. Tuinier, A Search for Natural Hydrophobic Deep Eutectic Solvents Based on Natural Components, *ACS Sustainable Chem. Eng.*, 2019, **7**, 2933–2942.

23 D. Dhingra, Bhawna, A. Pandey and S. Pandey, Fluorescence Quenching by Nitro Compounds within a Hydrophobic Deep Eutectic Solvent, *J. Phys. Chem. B*, 2020, **124**, 4164–4173.

24 P. Makoś, E. Słupek and J. Gębicki, Hydrophobic Deep Eutectic Solvents in Microextraction Techniques–A Review, *Microchem. J.*, 2020, **152**, 104384.

25 C. Florindo, L. C. Branco and I. M. Marrucho, Quest for Green-Solvent Design: From Hydrophilic to Hydrophobic (Deep) Eutectic Solvents, *ChemSusChem*, 2019, **12**, 1549–1559.

26 T. E. Phelps, N. Bhawawet, S. S. Jurisson and G. A. Baker, Efficient and Selective Extraction of $^{99m}TcO_4^-$ from Aqueous Media Using Hydrophobic Deep Eutectic Solvents, *ACS Sustainable Chem. Eng.*, 2018, **6**, 13656–13661.

27 D. J. G. P. Van Osch, J. Van Spronsen, A. C. C. Esteves, R. Tuinier and M. Vis, Oil-in-Water Emulsions Based on Hydrophobic Eutectic Systems, *Phys. Chem. Chem. Phys.*, 2020, **22**, 2181–2187.

28 R. Rai, S. Pandey, S. N. Baker, S. Vora, K. Behera, G. A. Baker and S. Pandey, Ethanol-Assisted, Few Nanometer, Water-In-Ionic-Liquid Reverse Micelle Formation by a Zwitterionic Surfactant, *Chem. – Eur. J*, 2012, **18**, 12213–12217.

29 R. Rai and S. Pandey, Evidence of Water-in-Ionic Liquid Microemulsion Formation by Nonionic Surfactant Brij-35, *Langmuir*, 2014, **30**, 10156–10160.

30 E. Bardez, B.-T. Goguillon, E. Keh and B. Valeur, Dynamics of Excited-State Reactions in Reversed Micelles. 1. Proton Transfer Involving a Hydrophilic Fluorescent Probe, *J. Phys. Chem.*, 1984, **88**, 1909–1913.

31 S. S. Mojumdar, T. Mondal, A. K. Das, S. Dey and K. Bhattacharyya, Ultrafast and Ultraslow Proton Transfer of Pyranine in an Ionic Liquid Microemulsion, *J. Chem. Phys.*, 2010, **132**, 194505–194513.

32 C. L. Costa Amaral, O. Brino, H. Chaimovich and M. J. Politi, Formation and Properties of Reversed Micelles of Aerosol OT Containing Urea in the Aqueous Pool, *Langmuir*, 1992, **8**, 2417–2421.

33 T. Htun, Excited-State Proton Transfer in Nonaqueous Solvents, *J. Fluoresc.*, 2003, **13**, 323–326.

34 R. Pramanik, S. Sarkar, C. Ghatak, V. G. Rao, P. Setua and N. Sarkar, Microemulsions with Surfactant TX100, Cyclohexane, and an Ionic Liquid Investigated by Conductance, DLS, FTIR Measurements, and Study of Solvent and Rotational Relaxation within this Microemulsion, *J. Phys. Chem. B*, 2010, **114**, 7579–7586.

35 M. Kaur, G. Singh, S. Kumar, Navnidhi and T. S. Kang, Thermally Stable Microemulsions Comprising Imidazolium Based Surface Active Ionic Liquids, Non-Polar Ionic Liquid and Ethylene Glycol as Polar Phase, *J. Colloid Interface Sci.*, 2018, **511**, 344–354.